

University of Wollongong  
**Research Online**

---

Australian Institute for Innovative Materials -  
Papers

Australian Institute for Innovative Materials

---

1-1-2013

## Ti substitution for Mn in MnCoGe - The magnetism of Mn<sub>0.9</sub>Ti<sub>0.1</sub>CoGe

Jianli Wang

*University of Wollongong*, [jianli@uow.edu.au](mailto:jianli@uow.edu.au)

P Shamba

*University of Wollongong*, [ps807@uowmail.edu.au](mailto:ps807@uowmail.edu.au)

W D. Hutchinson

*The University Of New South Wales*

M F. Md Din

*University of Wollongong*, [mfmd999@uowmail.edu.au](mailto:mfmd999@uowmail.edu.au)

J C. Debnath

*University Of Wollongong*, [jcd341@uow.edu.au](mailto:jcd341@uow.edu.au)

*See next page for additional authors*

Follow this and additional works at: <https://ro.uow.edu.au/aiimpapers>



Part of the [Engineering Commons](#), and the [Physical Sciences and Mathematics Commons](#)

---

### Recommended Citation

Wang, Jianli; Shamba, P; Hutchinson, W D.; Md Din, M F.; Debnath, J C.; Avdeev, M; Zeng, R; Kennedy, S J.; Campbell, S J.; and Dou, S X., "Ti substitution for Mn in MnCoGe - The magnetism of Mn<sub>0.9</sub>Ti<sub>0.1</sub>CoGe" (2013). *Australian Institute for Innovative Materials - Papers*. 782.  
<https://ro.uow.edu.au/aiimpapers/782>

Research Online is the open access institutional repository for the University of Wollongong. For further information contact the UOW Library: [research-pubs@uow.edu.au](mailto:research-pubs@uow.edu.au)

---

## Ti substitution for Mn in MnCoGe - The magnetism of Mn<sub>0.9</sub>Ti<sub>0.1</sub>CoGe

### Abstract

Bulk magnetization measurements (5-320 K; 0-8T) reveal that below room temperature Mn<sub>0.9</sub>Ti<sub>0.1</sub>CoGe exhibits two magnetic phase transitions at ~178 K and ~280 K. Neutron diffraction measurements (3-350K) confirm that the transition at ~178K is due to the structural change from the low-temperature orthorhombic TiNiSi-type structure to the higher temperature hexagonal Ni<sub>2</sub>In-type structure while the transition at ~280K originates from the transition from ferromagnetism to paramagnetism.

### Keywords

substitution, 9ti0, 1coge, mn, mncoge, magnetism, ti, mn0

### Disciplines

Engineering | Physical Sciences and Mathematics

### Publication Details

Wang, J. L., Shamba, P., Hutchinson, W. D., Md Din, M. F., Debnath, J. C., Avdeev, M., Zeng, R., Kennedy, S. J., Campbell, S. J. & Dou, S. X. (2013). Ti substitution for Mn in MnCoGe - The magnetism of Mn<sub>0.9</sub>Ti<sub>0.1</sub>CoGe. *Journal of Alloys and Compounds*, 577 (November), 475-479.

### Authors

Jianli Wang, P Shamba, W D. Hutchinson, M F. Md Din, J C. Debnath, M Avdeev, R Zeng, S J. Kennedy, S J. Campbell, and S X. Dou

Ti substitution for Mn in MnCoGe – The magnetism of Mn<sub>0.9</sub>Ti<sub>0.1</sub>CoGe

J.L. Wang<sup>1,2</sup>, P. Shamba<sup>1</sup>, W.D. Hutchison<sup>3</sup>, M.F. Md Din<sup>1</sup>, J. C. Debnath<sup>1,4</sup>, M. Avdeev<sup>2</sup>, R. Zeng<sup>1,5</sup>, S.J. Kennedy<sup>2</sup>, S.J. Campbell<sup>3</sup>, and S.X. Dou<sup>1</sup>

<sup>1</sup>Institute for Superconductivity and Electronic Materials, University of Wollongong, Wollongong, NSW 2522, Australia

<sup>2</sup>Bragg Institute, Australian Nuclear Science and Technology Organization, Lucas Heights, NSW 2234, Australia

<sup>3</sup>School of Physical, Environmental and Mathematical Sciences, The University of New South Wales, Canberra, ACT 2600, Australia

<sup>4</sup>Department of Physics, University of Johannesburg, PO Box 524, Auckland Park 2006, South Africa

<sup>5</sup>Solar Energy Technologies, School of Computing, Engineering and Mathematics, University of Western Sydney, Penrith South, Sydney, NSW 2751, Australia.

Bulk magnetization measurements (5 - 320 K; 0 – 8 T) reveal that below room temperature Mn<sub>0.9</sub>Ti<sub>0.1</sub>CoGe exhibits two magnetic phase transitions at ~178 K and ~280 K. Neutron diffraction measurements (3 – 350 K) confirm that the transition at ~178 K is due to the structural change from the low-temperature orthorhombic TiNiSi-type structure (space group Pnma) to the higher temperature hexagonal Ni<sub>2</sub>In-type structure (space group P63/mmc), while the transition at ~280 K originates from the transition from ferromagnetism to paramagnetism. The magnetocaloric behaviour of Mn<sub>0.9</sub>Ti<sub>0.1</sub>CoGe around T<sub>str</sub>~178 K and T<sub>C</sub>~280 K as determined *via* the magnetic field and temperature dependences of DC magnetisation are given by the maximum values of the magnetic entropy changes  $-\Delta S_M^{\max} = 6.6 \text{ J kg}^{-1} \text{ K}^{-1}$  around T<sub>str</sub>~178 K, and  $-\Delta S_M^{\max} = 4.2 \text{ J kg}^{-1} \text{ K}^{-1}$  around T<sub>C</sub>~280 K for a magnetic field change of  $\Delta B=0-8 \text{ T}$ . Both structural entropy - due to the unit cell expansion of ~4.04% - and magnetic entropy - due to an increase in the magnetic moment of ~31% - are

found to contribute significantly to the total entropy change around  $T_{\text{str}}$ . Critical analysis of the transition around  $T_C \sim 280$  K leads to exponents similar to values derived from a mean field theory, consistent with long-range ferromagnetic interactions. It was found that the field dependence of  $-\Delta S_M^{\text{max}}$  can be expressed as  $-\Delta S_M^{\text{max}} \propto B^n$  with  $n=1$  for the structural transition around  $T_{\text{str}}$  and  $n=2/3$  for the ferromagnetic transition around  $T_C$ , thereby confirming the second order nature of this latter transition.

Key Words: Magnetic phase transitions, magnetocaloric effect, Neutron diffraction in structure determination,

PACS: 75.30.Kz, 75.30.Sg 61.05.fm

## Introduction

Magnetic refrigeration (MR) based on the magnetocaloric effect (MCE) offers an environmentally friendly cooling technology with relatively high energy efficiency [1, 2]. Depending on the temperature of maximum entropy change, materials which exhibit a large magnetocaloric effect offer scope for magnetic refrigeration at cryogenic temperatures and around room temperature; as such they continue to attract significant interest and attention [e.g. 3, 4]. Materials with first-order magnetic phase transitions (FOMT) are of particular interest as the discontinuous character of the transition can lead to intrinsically large MCE values [5-7]. Among the relatively low-cost 3d metal-based compounds materials whose MCE response at such FOMT has been explored are  $\text{MnAs}_{1-x}\text{Sb}_x$  [7, 8],  $\text{MnFeP}_{0.45}\text{As}_{0.55}$  [9],  $\text{La}(\text{Fe}_{1-x}\text{Si}_x)_{13}$  and its hydrides [10, 11] as well as hexagonal  $\text{MnCoGe}/\text{MnNiGe}$ -based compounds [12, 13, 14].

Earlier studies of parent compound  $\text{MnCoGe}$  indicated that a martensitic structural transformation [15] from the low-temperature orthorhombic  $\text{TiNiSi}$ -type structure (space group  $\text{Pnma}$ ) to the high-temperature hexagonal  $\text{Ni}_2\text{In}$ -type structure (space group  $\text{P6}_3/\text{mmc}$ ) occurs at around  $T_{\text{str}}=650$  K. [16]. The orthorhombic  $\text{TiNiSi}$ -type structure of  $\text{MnCoGe}$  is reported to be ferromagnetic below the second-order paramagnetic to ferromagnetic transition at  $T_c\sim 345$  K while the hexagonal  $\text{Ni}_2\text{In}$ -type structure exhibits a ferromagnetic transition at  $T_c\sim 275$  K [16, 17]. Given that a large volume decrease of approximately 3.9% in  $\text{MnCoGe}$  compound occurs at  $T_{\text{str}}$  when the crystal symmetry changes from orthorhombic to hexagonal [15],  $\text{MnCoGe}$  and related compounds are of interest because of the scope to control the temperatures ( $T_{\text{str}}$  and  $T_c$  to coincide or be close enough) at which the magnetic and structural transitions occur and thereby capitalise on both magnetic and structural entropies. In this way a single first-order magnetostructural transition leading to an enhanced magnetocaloric effect near room temperature can be derived [12, 13, 18]. Recently, in order to realize the desired

magnetostructural coupling, lots of efforts have been made in different ways to modify the MnCoGe/MnNGe compositions [12-13, 18-24] .

Our recent investigation [25] of  $\text{Mn}_{0.94}\text{Ti}_{0.06}\text{CoGe}$  indicates that a small amount of Ti leads to a significant decrease in  $T_{\text{str}}$ ; for example  $T_{\text{str}}=235$  K for  $\text{Mn}_{0.94}\text{Ti}_{0.06}\text{CoGe}$  compared with  $T_{\text{str}}=645$  K for MnCoGe. In order to fully understand the effects of Ti substitution for Mn on the magnetic and structural properties of  $\text{Mn}_{1-x}\text{Ti}_x\text{CoGe}$ , here we present the results of a detailed investigation of the structural and magnetic properties of  $\text{Mn}_{0.9}\text{Ti}_{0.1}\text{CoGe}$  (where both  $T_{\text{str}}$  and  $T_{\text{C}}$  are shifted into our interested temperature range) by dc magnetization, x-ray and neutron diffraction measurements.

### Experiment process

The  $\text{Mn}_{0.9}\text{Ti}_{0.1}\text{CoGe}$  sample was prepared by argon arc melting appropriate amounts of high purity elements on a water-cooled Cu hearth. Around ~3% excess Mn was used to compensate for loss during melting. The sample was re-melted five times to ensure good homogeneity and annealed at 850°C for one week in an evacuated quartz tube then quenched into water. X-ray diffraction ( $\text{CuK}_{\alpha}$ ) at room temperature confirmed that the sample exhibited the hexagonal  $\text{Ni}_2\text{In}$ -type structure (space group  $P6_3/mmc$ ) with no discernible impurity phases. The magnetic measurements were carried out using a Physical Property Measurement System over the temperature range 5-320 K and at magnetic fields in the range 0-8 T. Neutron diffraction experiments were carried out over the temperature range 3 – 350 K using the High-Resolution Powder Diffractometer Echidna ( $\lambda = 1.622$  Å) at the OPAL reactor, Australia. The diffraction patterns were refined using the FULLPROF program package which allows simultaneous refinement of the structural and magnetic parameters.

### Results and Discussion

Figure 1(a) shows the temperature dependence of the magnetization of  $\text{Mn}_{0.9}\text{Ti}_{0.1}\text{CoGe}$  obtained at magnetic fields  $B=0.01$  T,  $B=0.1$  T and  $B=4$  T. Two magnetic phase transitions can be discerned at  $\sim 178$  K and  $\sim 280$  K (see also the insert to Figure 1(a) which displays the  $B=0.01$  T data on an expanded temperature range). Based on the analogous magnetic behaviour between  $\text{Mn}_{0.9}\text{Ti}_{0.1}\text{CoGe}$  and  $\text{Mn}_{0.94}\text{Ti}_{0.06}\text{CoGe}$  [25], these transitions can be ascribed as representing the orthorhombic to hexagonal structure at  $T_{\text{str}} \sim 178$  K with  $T_{\text{C}} \sim 280$  K indicating the paramagnetic to ferromagnetic transition in the hexagonal phase. As discussed further below, Fig. 1(a) also reveals a significant decrease in the magnetization data obtained for  $B=4$  T around  $T_{\text{str}} \sim 178$  K. Fig. 1(b) shows the magnetization data for  $\text{Mn}_{0.9}\text{Ti}_{0.1}\text{CoGe}$  in the region of the transitions at  $T_{\text{str}} \sim 178$  K and  $T_{\text{C}} \sim 280$  K as obtained from 140 K to 320 K in 5 K increments for increasing and decreasing magnetic fields in the range  $B = 0-8$  T with the corresponding Arrott-plots of  $M^2$  versus  $B/M$  shown in Fig. 1(c).

Fig. 2(a) shows the spontaneous magnetization  $M_{\text{s}}$  for  $\text{Mn}_{0.9}\text{Ti}_{0.1}\text{CoGe}$  as a function of temperature as derived from Figs. 1(b) and 1(c). Below  $T_{\text{str}}$  in the orthorhombic phase, e.g. at  $T=150$  K, the spontaneous magnetization  $M_{\text{s}} = 97.3$  Am<sup>2</sup>/kg corresponds to a magnetic moment of  $\sim 3.24 \mu_{\text{B}}$ , while above  $T_{\text{str}}$  in the hexagonal phase, e.g. at  $T=200$  K, the value of  $M_{\text{s}} = 67.6$  Am<sup>2</sup>/kg is equivalent to a magnetic moment of  $\sim 2.29 \mu_{\text{B}}$ . These changes reflect a decrease in spontaneous magnetization  $M_{\text{s}}$  of about  $\sim 31\%$  around the transition  $T_{\text{str}}$  from the orthorhombic structure to the hexagonal structure, which agrees well with the fact that the Mn and Co atoms in the TiNiSi-structure have larger magnetic moments than with Ni<sub>2</sub>In-type based on *ab initio* total energy calculations for MnCoGe [26] and  $\text{MnCo}_{1-x}\text{Ge}$  compounds [17]. Comparison of the temperature  $T_{\text{str}}$  at which the low-temperature orthorhombic structure (space group Pnma) changes to the hexagonal structure (space group P63/mmc) for the undoped MnCoGe compound [ $T_{\text{str}} \sim 645$  K; 16],  $\text{Mn}_{0.94}\text{Ti}_{0.06}\text{CoGe}$  [ $T_{\text{str}} \sim 235$  K; 25] and  $\text{Mn}_{0.9}\text{Ti}_{0.1}\text{CoGe}$  sample [ $T_{\text{str}} \sim 178$  K; present results] demonstrates that substitution of Ti for

Mn extends the phase stability region of the hexagonal P63/mmc structure significantly to lower temperatures.

The positive slopes of the Arrott plots for  $\text{Mn}_{0.9}\text{Ti}_{0.1}\text{CoGe}$  around  $T_C \sim 280$  K as outlined above, Fig. 1(c), indicate that the magnetic transition around  $T_C$  is second order. According to the conventional static scaling law, the critical properties of a second-order magnetic transition can be described by critical exponents  $\beta$ ,  $\gamma$  and  $\delta$  derived from magnetization measurements around the transition temperature [e.g. 25, 27]. On applying these standard approaches, as shown by the fits to the Kouvel-Fisher plots of  $M_s(T)(dM_s/dT)^{-1}$  and  $\chi_0^{-1}(T)(d\chi_0/dT)^{-1}$  versus temperature in Fig. 2(b), the critical exponents around  $T_C$  in  $\text{Mn}_{0.9}\text{Ti}_{0.1}\text{CoGe}$  have been determined to be  $\beta=0.45$  and  $\gamma=0.83$ . Hence, on applying the relationship  $\delta = 1 + \gamma/\beta$ , with  $\beta = 0.45$ ,  $\gamma = 0.83$ , the critical exponent  $\delta = 1 + \gamma/\beta = 2.84$ . The critical exponents determined for  $\text{Mn}_{0.9}\text{Ti}_{0.1}\text{CoGe}$  -  $\beta = 0.45$ ,  $\delta = 2.84$  and  $\gamma = 0.83$  - are similar to the theoretical values of the mean-field model for which  $\beta=0.5$ ,  $\delta=3.0$  and  $\gamma=1.0$ , consistent with the existence of a long-range ferromagnetic interactions [27].

Figure 3(a) shows neutron diffraction patterns collected at  $T=3$  K, 150 K, 200 K, 300 K and 350 K; these temperatures were selected in order to investigate the crystallographic and magnetic structures of  $\text{Mn}_{0.9}\text{Ti}_{0.1}\text{CoGe}$  around the transition temperatures  $T_{\text{str}} \sim 178$  K and  $T_C \sim 280$  K. Refinements confirm that at 300 K and 350 K (i.e. above  $T_C = 280$  K), the sample crystallizes in the hexagonal  $\text{Ni}_2\text{In}$ -type structure of P63/mmc space group and is in the paramagnetic state. By comparison at 200 K, while the crystal structure remains hexagonal, the enhanced magnetic scattering (e.g. the (100) and (110) Reflections) confirms that at 200 K  $\text{Mn}_{0.9}\text{Ti}_{0.1}\text{CoGe}$  is ferromagnetic. Refinement of the 200 K pattern (Fig. 3(a)) leads to magnetic moment values of  $\mu(\text{Mn})=2.3 \mu_B$  and  $\mu(\text{Co})=0.6 \mu_B$  - total moment  $\mu^{\text{tot}}= 2.9 \mu_B$  for the hexagonal structure of  $\text{Mn}_{0.9}\text{Ti}_{0.1}\text{CoGe}$  at 200 K, which is quite close to the value of  $M_s$  ( $2.3 \mu_B$ ) derived from magnetic measurement above.



As further indicated by the refinement of the diffraction pattern of Fig. 3(a) at 150 K, i.e. below  $T_{\text{str}} \sim 178$  K, on decreasing the temperature below  $T_{\text{str}}$ , the structure changes from single phase hexagonal to co-existence of the hexagonal  $\text{Ni}_2\text{In}$ -type structure (P63/mmc) of phase fraction 54(2)% and the orthorhombic  $\text{TiNiSi}$ -type structure (space group Pnma) of phase fraction 46(2)%. Given the large number of fitted parameters introduced constraints during the refinements, we assume that the atomic magnetic moments of P63/mmc phase remain constant in the magnetic region. The resultant magnetic moments for the Pnma phase are  $\mu(\text{Mn})=3.1 \mu_{\text{B}}$  and  $\mu(\text{Co})=0.9 \mu_{\text{B}}$  at 150 K, thus indicating the orthorhombic structure has a higher magnetic moment than the hexagonal structure, as expected by *ab initio* total energy calculations [17, 26] and agreeing well with our magnetic measurements mentioned above (Fig. 1(b)). This behaviour, with the moment in the orthorhombic phase larger than that in the hexagonal phase, is similar to that reported for the parent  $\text{MnCoGe}$  compound in which the value of the saturation moment for the orthorhombic structure is  $M_{\text{S}}^{\text{orth}} = 4.13 \mu_{\text{B}}$  [16] while in the hexagonal structure,  $M_{\text{S}}^{\text{hex}} = 2.76 \mu_{\text{B}}$  [28]. Refinement of the neutron diffraction pattern at 3 K (Fig. 3(a)), shows the fraction of the hexagonal P63/mmc phase has decreased to 43(1)% with the orthorhombic Pnma phase increasing to 57(1)%. In the case of  $\text{Mn}_{0.94}\text{Ti}_{0.06}\text{CoGe}$ , however, it was found that below  $T_{\text{str}}$  (at  $\sim 235$  K, [25]) the  $\text{Mn}_{0.94}\text{Ti}_{0.06}\text{CoGe}$  phase exhibits 100% of the orthorhombic  $\text{TiNiSi}$ -type structure. So, it indicates again that the stability of hexagonal P63/mmc phase is enhanced due to the substitution of Ti for Mn.

Fig. 3(b) shows the temperature dependence of the lattice parameters and unit cell volumes together with the fractions of the hexagonal and orthorhombic phases of  $\text{Mn}_{0.9}\text{Ti}_{0.1}\text{CoGe}$  as derived from refinements of the neutron data. In order to compare directly, we modify the lattice parameters of orthorhombic and hexagonal structures using the relationships  $a_{\text{ortho}}=c_{\text{hex}}$ ,  $b_{\text{ortho}}=a_{\text{hex}}$ ,  $c_{\text{ortho}}=_3a_{\text{hex}}$ , and  $V_{\text{ortho}}=2V_{\text{hex}}$  [15]. As is evident from Fig. 3(b), the

change in crystal structure from hexagonal P63/mmc to orthorhombic Pnma is associated with an increment in the unit cell volume of around ~4.04 percent. The change in unit cell volume, similar to that observed in Mn<sub>1.07</sub>Co<sub>0.92</sub>Ge for which a change of  $\Delta V/V \sim 5.3\%$ , was obtained around  $T_{\text{str}} \sim 210$  K [29].

The isothermal entropy change corresponding to magnetic field change  $\Delta B$  (starting from zero field) can be conveniently derived from the magnetization data using the Maxwell relation [e.g. 2–6]:

$$\Delta S_M(T, B) = \int_0^B \left( \frac{\partial M(T, B)}{\partial T} \right)_B dB \quad (1).$$

Use of the Maxwell relation (Eqn. (1)) in determining  $\Delta S_M$  from first order magnetic transition (FOMT) has been discussed thoroughly in the literature [e.g. 1, 3, 30-32]; this has led to deep insight to the suitability of different experimental and related analytical approaches in order to establish the isothermal entropy change. In the case of Mn<sub>0.9</sub>Ti<sub>0.1</sub>CoGe, the absence of field hysteresis in the magnetisation data around  $T_{\text{str}}$  (see Fig. 1(b)), indicates that this Maxwell method can be applied to determining the entropy change around  $T_{\text{str}}$ . The temperature dependence of the magnetic entropy changes in the region of  $T_{\text{str}} \sim 178$  K and  $T_C \sim 280$  K are shown in Fig. 4(a) with the curves for decreasing field and increasing field found to be essentially identical. Fig. 4(a) also reveals that the entropy change is significantly higher at  $T_{\text{str}}$  of maximum value  $-\Delta S_M^{\text{max}} \sim 6.6$  J/kg K, compared with the value at  $T_C$  of  $-\Delta S_M^{\text{max}} \sim 4.2$  J/kg K for a field change of  $\Delta B = 8$  T. Fig. 4(b) shows the maximum values derived for the entropy change  $-\Delta S_M^{\text{max}}$  around  $T_{\text{str}}$  and  $T_C$  as a function of magnetic field values, it can be seen clearly that with increasing field, the value of  $\Delta S_M^{\text{max}}$  around  $T_{\text{str}}$  increases much faster than around  $T_C$ . As shown by the fit to the  $-\Delta S_M^{\text{max}}$  values around  $T_C$  in Fig. 4(b), the data at the ferromagnetic transition can be well described by the functional form  $-\Delta S_M^{\text{max}} \propto B^{2/3}$  [33]. This behaviour confirms the second-order character of

the phase transition around  $T_C$  as concluded from analysis of the Arrott plots of Fig. 1(c). On the other hand, it was found that in the region around the structural transformation at  $T_{str} \sim 178$  K, the maximum values of the entropy change  $-\Delta S_M^{max}$  vary linearly with magnetic field, indicating the existence of the proportional relationship  $-\Delta S_M^{max} \propto B$  at this transition. It is well accepted that the total entropy can be written as sum of magnetic, lattice and electronic entropies. In general, all three contributions depend on temperature and magnetic field and cannot be clearly separated. Compared with the transition around  $T_C$ , the total entropy for the phase transition around  $T_{str}$  should be expected coming from two major contributions: (1) magnetic part due to the magnetization drop (the  $M_s$  difference in orthorhombic structure and in the hexagonal structure); (2) lattice entropy change due to the crystal structure change from orthorhombic Pnma to hexagonal P63/mmc with a  $\sim 4.04$  percent decrease in the unit cell volume, which is significant based on ref [34] where it was concluded that lattice entropy is proportional to the difference of phase volumes for the two phases involved in the first-order transformation.

## Conclusions

The structural and magnetic properties of  $Mn_{0.9}Ti_{0.1}CoGe$  compound have been investigated by magnetic (5 - 320 K; 0 – 8 T) and neutron diffraction (3 – 350 K) measurements. Substitution of Ti for Mn in the parent MnCoGe compound leads to a significant reduction in both  $T_{str}$  (from  $\sim 645$  K for MnCoGe to  $\sim 178$  K for  $Mn_{0.9}Ti_{0.1}CoGe$ ) and  $T_C$  (from  $\sim 345$  K for MnCoGe to  $\sim 280$  K for  $Mn_{0.9}Ti_{0.1}CoGe$ ).  $Mn_{0.9}Ti_{0.1}CoGe$  exhibits a single phase with the hexagonal  $Ni_2In$ -type structure above  $T_{str} \sim 178$  K while below  $T_{str}$  the hexagonal structure is found to co-exist with the orthorhombic  $TiNiSi$ -type structure, leading to phase fractions of 43(1)% and 58(1)% respectively at 3 K. The unit cell volume is found to expand around 4% on cooling below  $T_{str} \sim 178$  K along with an increase in magnetic moment of around 31%.

The field dependence of the maximum of magnetic entropy change  $\Delta S_M^{max}$  around  $T_C$  can be expressed as  $\Delta S_M^{max} \propto B^{2/3}$  as expected for a second order magnetic transition while the relationship  $\Delta S_M^{max} \propto B$  applies around the structural transition temperature  $T_{str}$ , which may be ascribed to the lattice entropy contribution.

## References

- [1] K. A. Gschneidner Jr, V. K. Pecharsky and A. O. Tsokol, *Rep. Prog. Phys.*, 68 (2005) 1479
- [2] E. Brück, O. Tegus, D. T. Cam Thanh, N. T. Trung and K. H. J. Buschow, *Int. J. Refrig.*, 31 (2008) 767.
- [3] A. M. Tishin and Y. Spichkin, *The Magnetocaloric Effect and its Applications*, Institute of Physics, Bristol, 2003
- [4] A. Smith, C. R. H. Bahl, R. Bjørk, K. Engelbrecht, K. K. Nielsen and N. Pryds, *Advanced Materials*, 2 (2012) 1288
- [5] V. K. Pecharsky and K. A. Gschneidner, *Phys. Rev. Lett.*, 78 (1997) 4494.
- [6] J.L. Wang, S.J. Campbell, J.M. Cadogan, A. Studer, R. Zeng and S.X. Dou, *Appl. Phys. Lett.*, 98 (2011) 232509;  
J. L.Wang, S. J. Kennedy, S. J. Campbell, M. Hofmann and S. X. Dou, *Phys. Rev. B*, 87 (2013) 104401;  
J. L. Wang, L. Caron, S. J. Campbell, S. J. Kennedy, M. Hofmann, Z. X. Cheng, M. F. Md Din, A. J. Studer, E. Brück, and S. X. Dou, *Phys. Rev. Lett.*, 110 (2013) 217211
- [7] H. Wada and Y. Tanabe, *Appl. Phys. Lett.*, 79 (2001) 3302.
- [8] H. Wada, T. Morikawa, K. Taniguchi, T. Shibata, Y. Yamada, and Y. Akishige, *Physica B*, 328 (2003) 114.

- [9] O. Tegus, E. Brück, K. H. J. Buschow and F. R. de Boer, *Nature* (London), 415 (2002) 150.
- [10] F.X. Hu, B.G. Shen, J.R. Sun, Z. Cheng, G. Rao, and X. Zhang, *Appl. Phys. Lett.*, 78, (2001) 3675.
- [11] A. Fujita, S. Fujieda, Y. Hasegawa and K. Fukamichi, *Phys. Rev. B*, 67 (2003) 104416.
- [12] N.T. Trung, V. Biharie, L. Zhang, L. Caron, K. H. J. Buschow and E. Brück, *Appl. Phys. Lett.*, 96 (2010) 162507
- [13] L. Caron, N. T. Trung and E. Brück, *Phys. Rev. B*, 84 (2011) 020414(R).
- [14] E.K. Liu, W.H. Wang, L. Feng, W. Zhu, G.J. Li, J.L. Chen, H.W. Zhang, G.H. Wu, C.B. Jiang, H.B. Xu and F.R. de Boer, *Nat. Commun.*, 3:873 doi: 10.1038/ncomms1868 (2012).
- [15] V. Johnson, *Inorg. Chem.*, 14 (1975) 1117.
- [16] T. Kanomata, H. Ishigaki, T. Suzuki, H. Yoshida, S. Abe, and T. Kaneko, *J. Magn. Magn. Mater.*, 140-144 (1995) 131.
- [17] J.T. Wang, D. S. Wang, C. Chen, O. Nashima, T. Kanomata, H. Mizuseki and Y. Kawazoe, *Appl. Phys. Lett.*, 89 (2006) 262504.
- [18] S. Lin, O. Tegus, E. Brück, W. Dagula, T. J. Gortenmulder and K.H.J. Buschow, *IEEE Trans. Magn.*, 42 (2006) 3776
- [19] C. L. Zhang, D. H. Wang, Q. Q. Cao, Z. D. Han, H. C. Xuan, and Y. W. Du, *Appl. Phys. Lett.*, 93(2008) 122505
- [20] N. T. Trung, L. Zhang, L. Caron, K. H. J. Buschow, and E. Brück, *Appl. Phys. Lett.*, 96 (2010) 172504
- [21] T. Samanta, I. Dubenko, A. Quetz, S. Temple, S. Stadler and N. Ali, *Appl. Phys. Lett.*, 100 (2012) 052404

- [22] T. Samanta, I. Dubenko, A. Quetz, S. Stadler and N. Ali, *Appl. Phys. Lett.*, 101 (2012) 242405
- [23] E. K. Liu, H. G. Zhang, G. Z. Xu, X. M. Zhang, R. S. Ma, W. H. Wang, J. L. Chen, H. W. Zhang, G. H. Wu, L. Feng and X. X. Zhang, *Appl. Phys. Lett.*, 102 (2013) 122405;
- [24] J.C. Debnath, P. Shamba, A.M. Strydom, J.L. Wang, and S.X. Dou, *J. Appl. Phys.*, 113 (2013) 093902
- [25] P. Shamba, J.L. Wang, J.C. Debnath, S.J. Kennedy, R. Zeng, M.F. Md Din, F. Hong, Z.X. Cheng, A.J. Studer and S.X. Dou, *J. Phys.: Condens. Matter.*, 25 (2013) 056001
- [26] S. Kaprzyk and S. Niziol, *J. Magn. Magn. Mater.*, 87 (1990) 267.
- [27] J.L. Wang, S.J. Campbell, S.J. Kennedy, R. Zeng, S.X. Dou and G.H. Wu, *J. Phys.: Condens. Matter.*, 23 (2011) 216002
- [28] T. Kanomata, H. Ishigaki, K. Sato, T. Shinohara, F. Wagatsuma, and T. Kaneko, *J. Magn. Soc. Jpn.* 23, 418 (1999).
- [29] K. Koyama, M. Saka, T. Kanomata and K. Watanabe, *Jpn. J. Appl. Phys.* 43 (2004) 8036
- [30] A. Giguère, M. Földeaki, B. Ravi Gopal, R. Chahine, T. K. Bose, A. Frydman, and J. A. Barclay, *Phys. Rev. Lett.*, 83 (1999) 2262.
- [31] F. Casanova, X. Batlle, A. Labarta, J. Marcos, L. Mañosa, and A. Planes, *Phys. Rev. B*, 66 (2002) 100401R.
- [32] L. Tocado, E. Palacios and R. Burriel, *J. Appl. Phys.*, 105 (2009) 093918.
- [33] V. Franco, J. S. Blázquez, and A. Conde, *Appl. Phys. Lett.*, 98 (2011) 232509
- [34] K. A. Gschneidner Jr., Y. Mudryk and V.K. Pecharsky, *Scripta Materialia*, 67 (2012) 572

Figure captions

Fig. 1 (a) Temperature dependence of the magnetization of  $\text{Mn}_{0.9}\text{Ti}_{0.1}\text{CoGe}$  as measured in the magnetic fields indicated ( $B=0.01$  T,  $0.1$  T and  $4$  T). The inset of Fig. 1(a) shows the expanded temperature range for  $B=0.01$  T; the transition temperatures  $T_{\text{str}}$  and  $T_{\text{C}}$  are marked by arrows; (b) Temperature dependence of magnetization for  $\text{Mn}_{0.9}\text{Ti}_{0.1}\text{CoGe}$  ( $B = 0-8$  T) as measured at various temperatures around  $T_{\text{str}}$  and  $T_{\text{C}}$ , and (c) the corresponding Arrott plots of  $M^2$  vs  $B/M$  as determined from the data of Fig. 1(b).

Fig. 2 (a) Spontaneous magnetization values  $M_{\text{s}}$  for  $\text{Mn}_{0.9}\text{Ti}_{0.1}\text{CoGe}$  as a function of temperature as derived from Figs. 1(b) and 1(c). (b) Kouvel-Fisher plots of  $M_{\text{s}}(T)(dM_{\text{s}}/dT)^{-1}$  (*left scale*) and  $\chi_0^{-1}(T)(d\chi_0/dT)^{-1}$  (*right scale*) versus temperature. The lines are fits to the data around  $T_{\text{C}}$  as discussed in the text with fits leading to the critical exponent values  $\beta = 0.45$ ,  $\gamma = 0.83$ , and hence  $\delta = 1 + \gamma/\beta = 2.84$ .

Fig. 3 (a) Neutron diffraction patterns of  $\text{Mn}_{0.9}\text{Ti}_{0.1}\text{CoGe}$  at  $T=3$  K,  $150$  K,  $200$  K,  $300$  K and  $350$  K ( $\lambda = 1.622$  Å). The full lines through the data represent Rietveld refinements to the hexagonal  $\text{Ni}_2\text{In}$ -type structure (P63/mmc; upper set of markers) and the orthorhombic  $\text{TiNiSi}$ -type structure (space group Pnma; lower set of markers) as discussed in the text. (b) The unit cell volumes and lattice parameters together with the fractions of the hexagonal and orthorhombic phases of  $\text{Mn}_{0.9}\text{Ti}_{0.1}\text{CoGe}$  as a function of temperature.

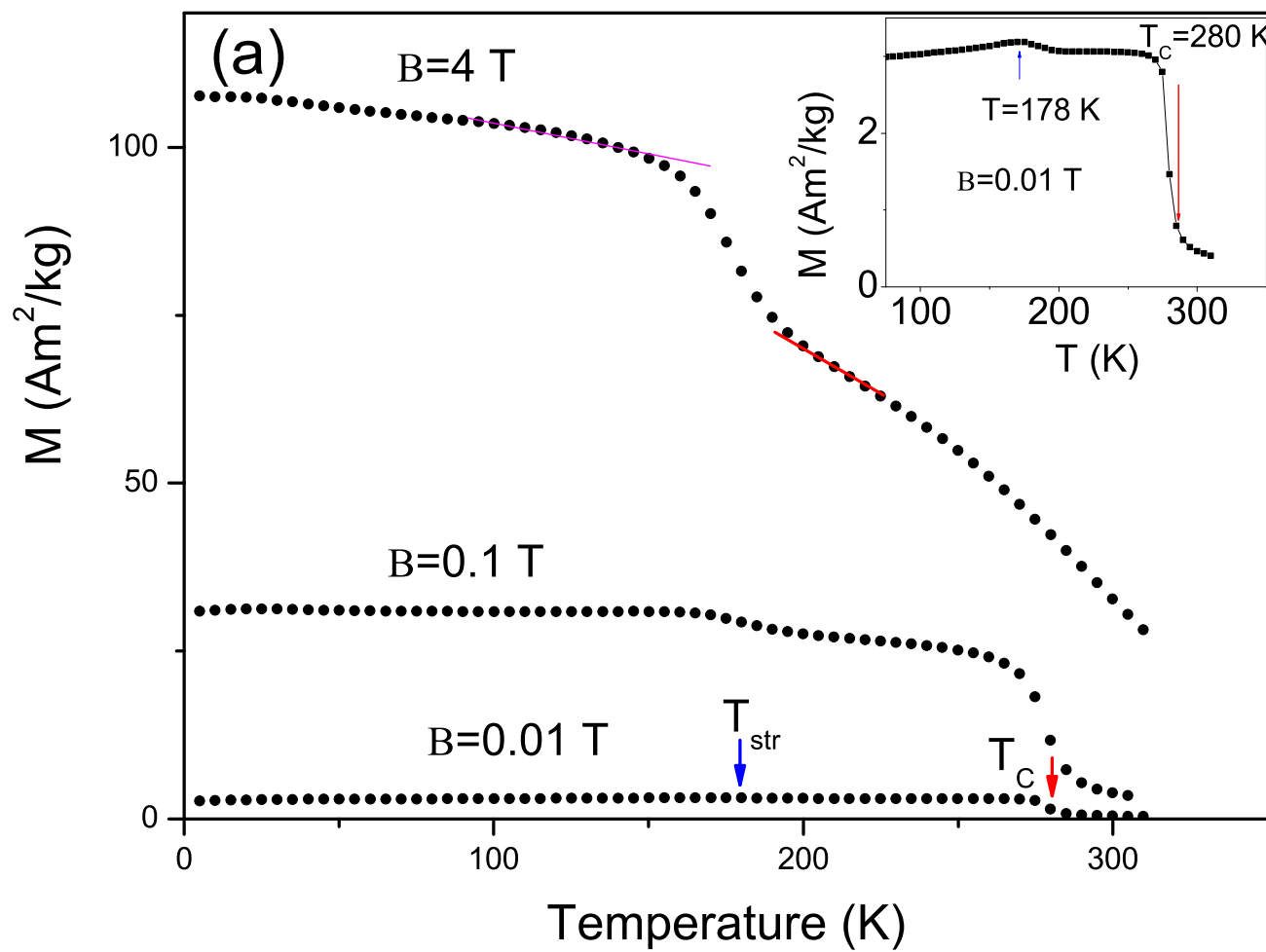
Fig. 4 (a) Temperature dependence of the isothermal magnetic entropy change  $-\Delta S_{\text{M}}(T, B)$  as calculated from the magnetization isotherms; (b) Graphs of the maximum values of the magnetic entropy change  $-\Delta S_{\text{M}}^{\text{max}}$  in the region of  $T_{\text{str}} \sim 178$  K and  $T_{\text{C}} \sim 280$  K as

functions of magnetic field  $B$ . The dashed lines represent fits to these data as discussed in the text.

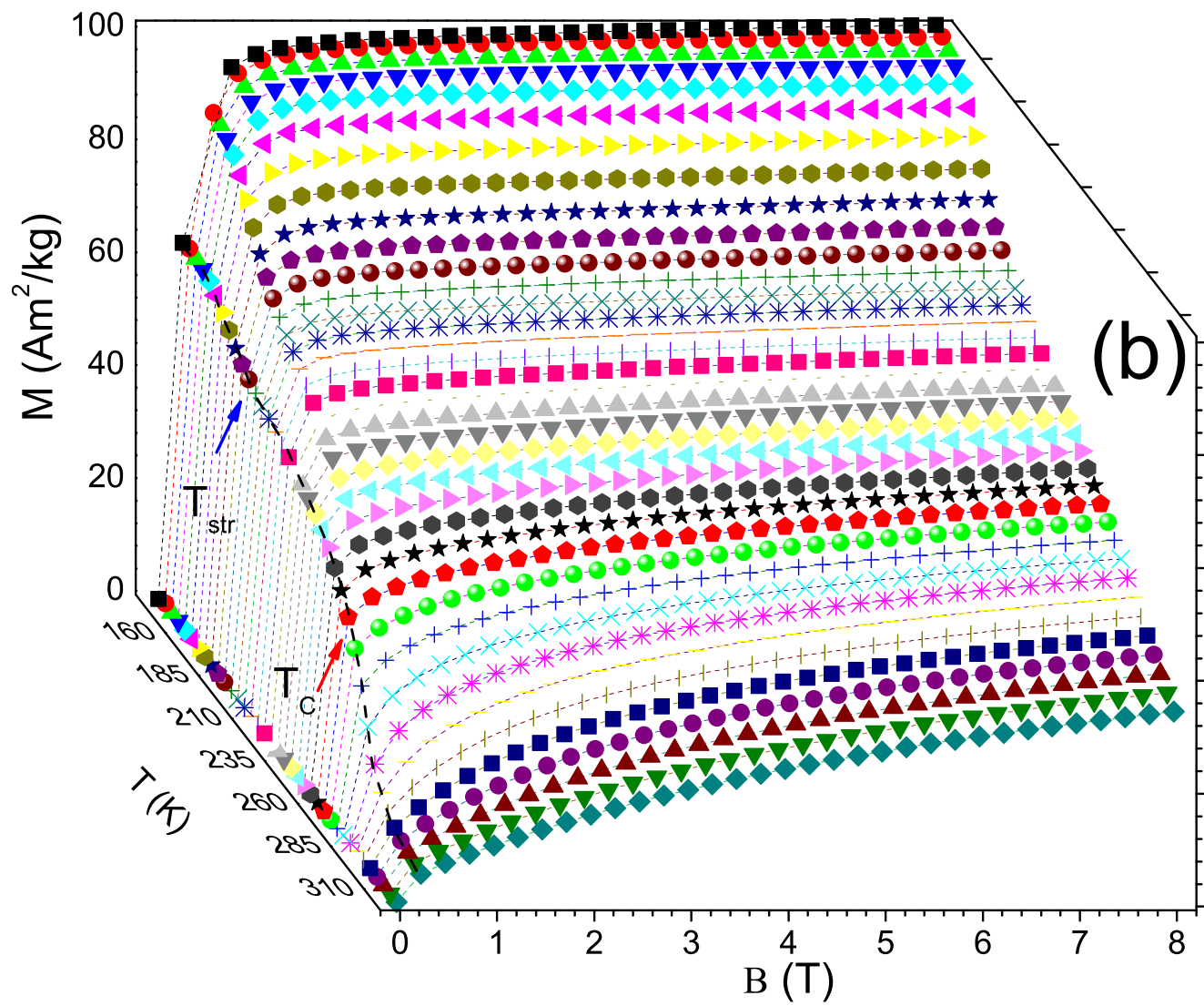


## \*Highlights (for review)

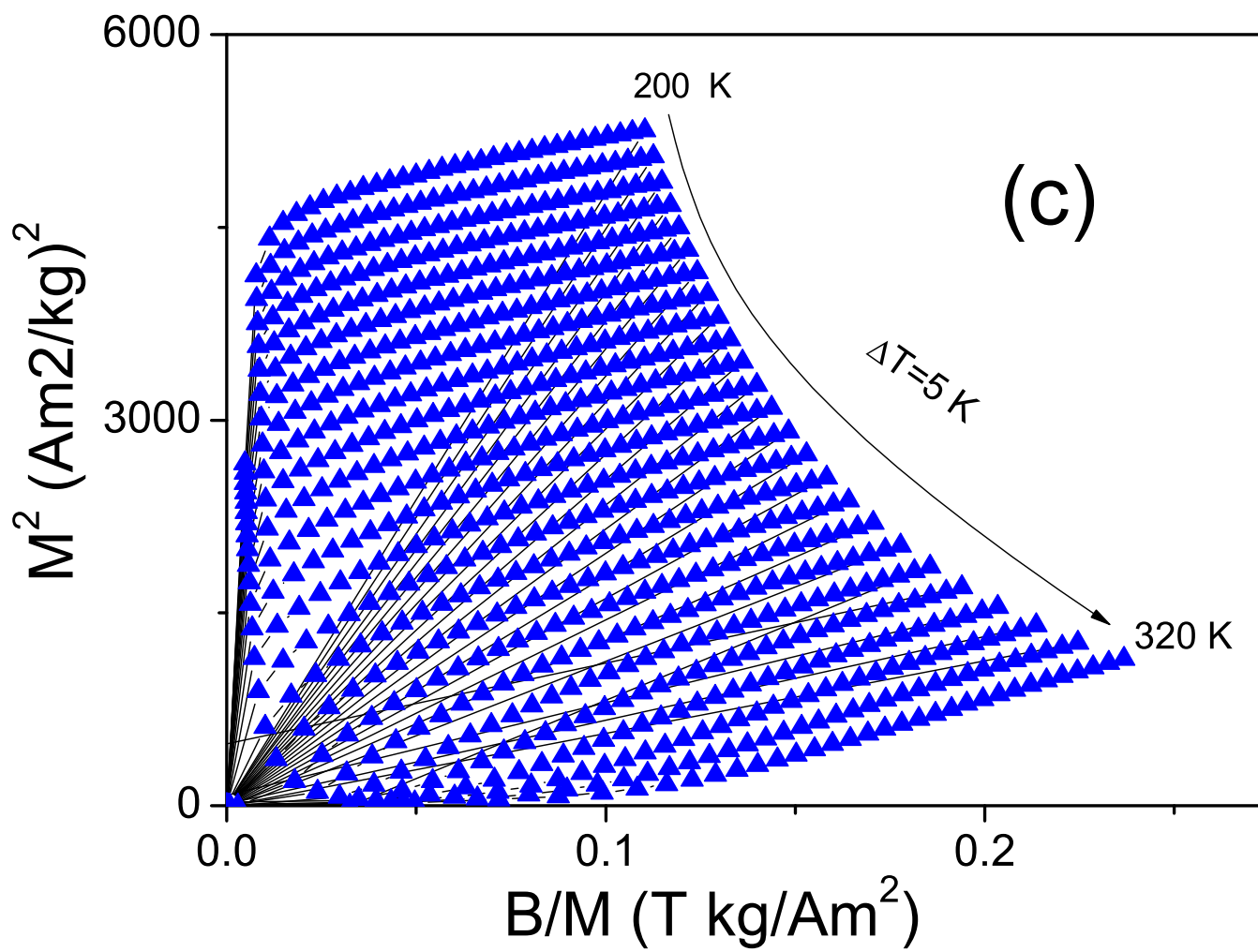
- We detected and confirmed two magnetic phase transitions at ~178 K and ~280 K
- Both structural entropy and magnetic entropy contribute to the entropy change around  $T_{\text{str}}$ .
- $-\Delta S_{\text{M}}^{\text{max}}$  can be expressed as  $-\Delta S_{\text{M}}^{\text{max}} \propto B^n$  with  $n=1$  around  $T_{\text{str}}$  and  $n=2/3$  around  $T_{\text{C}}$ .

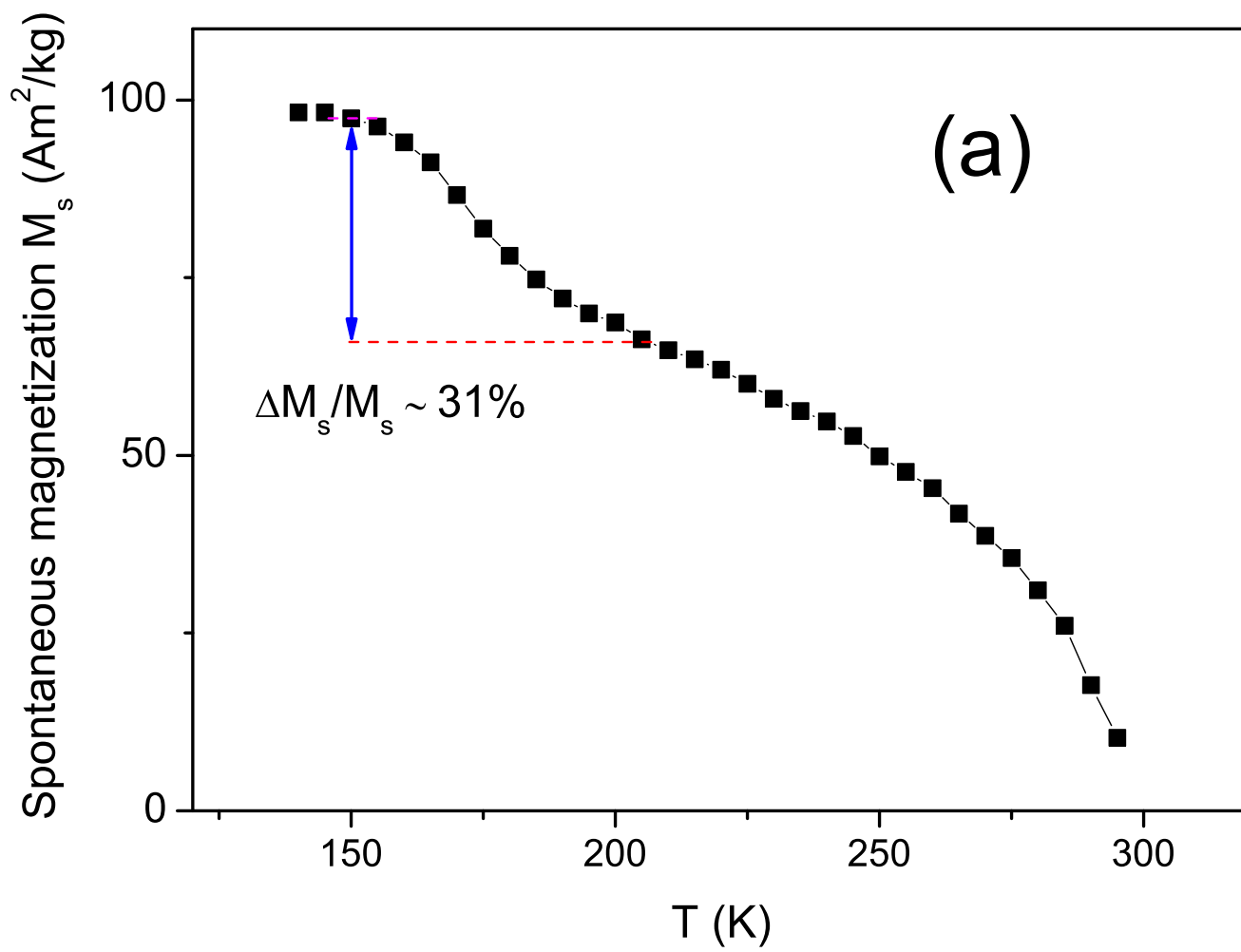


Figure(s)

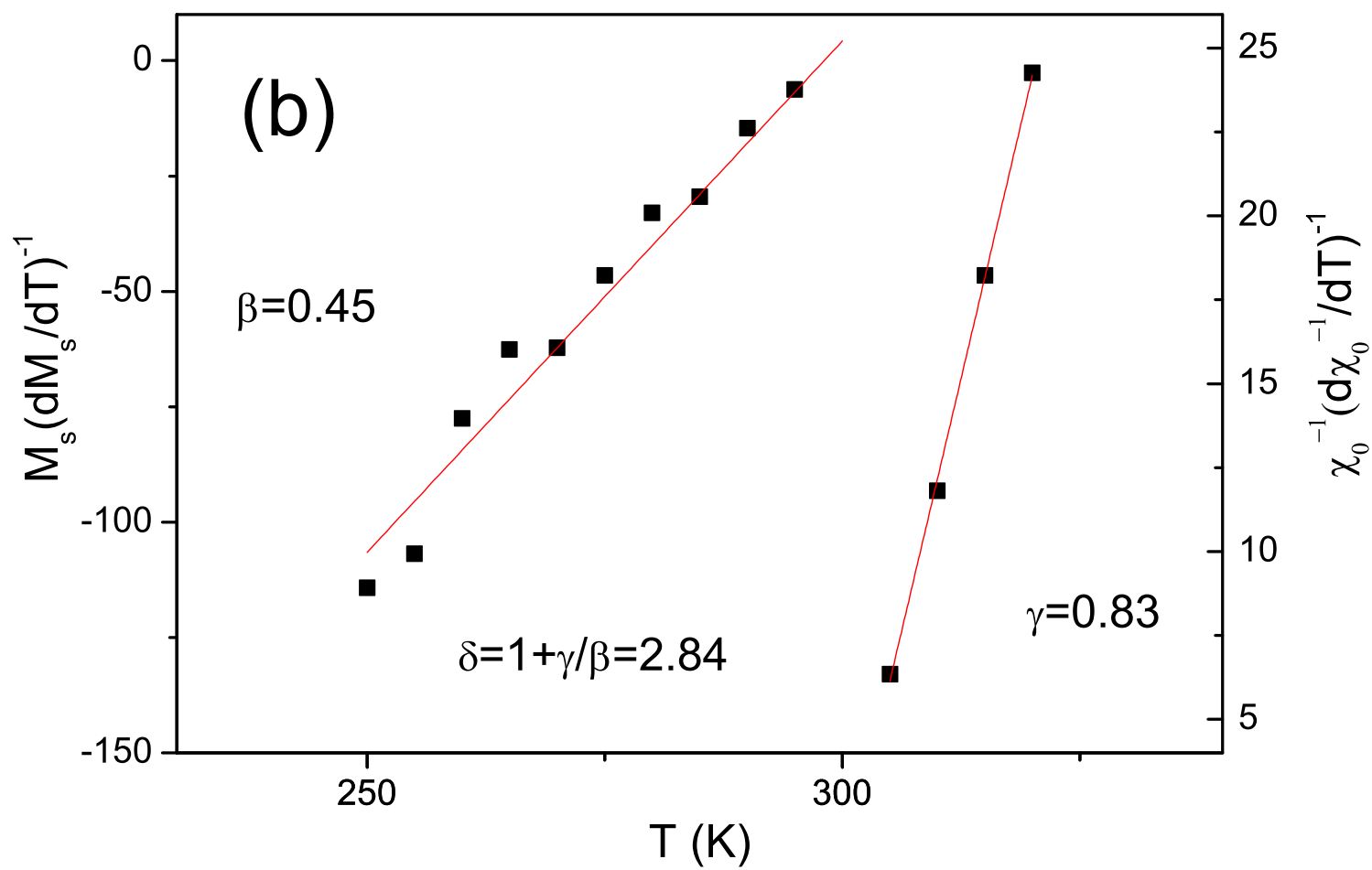


Figure(s)

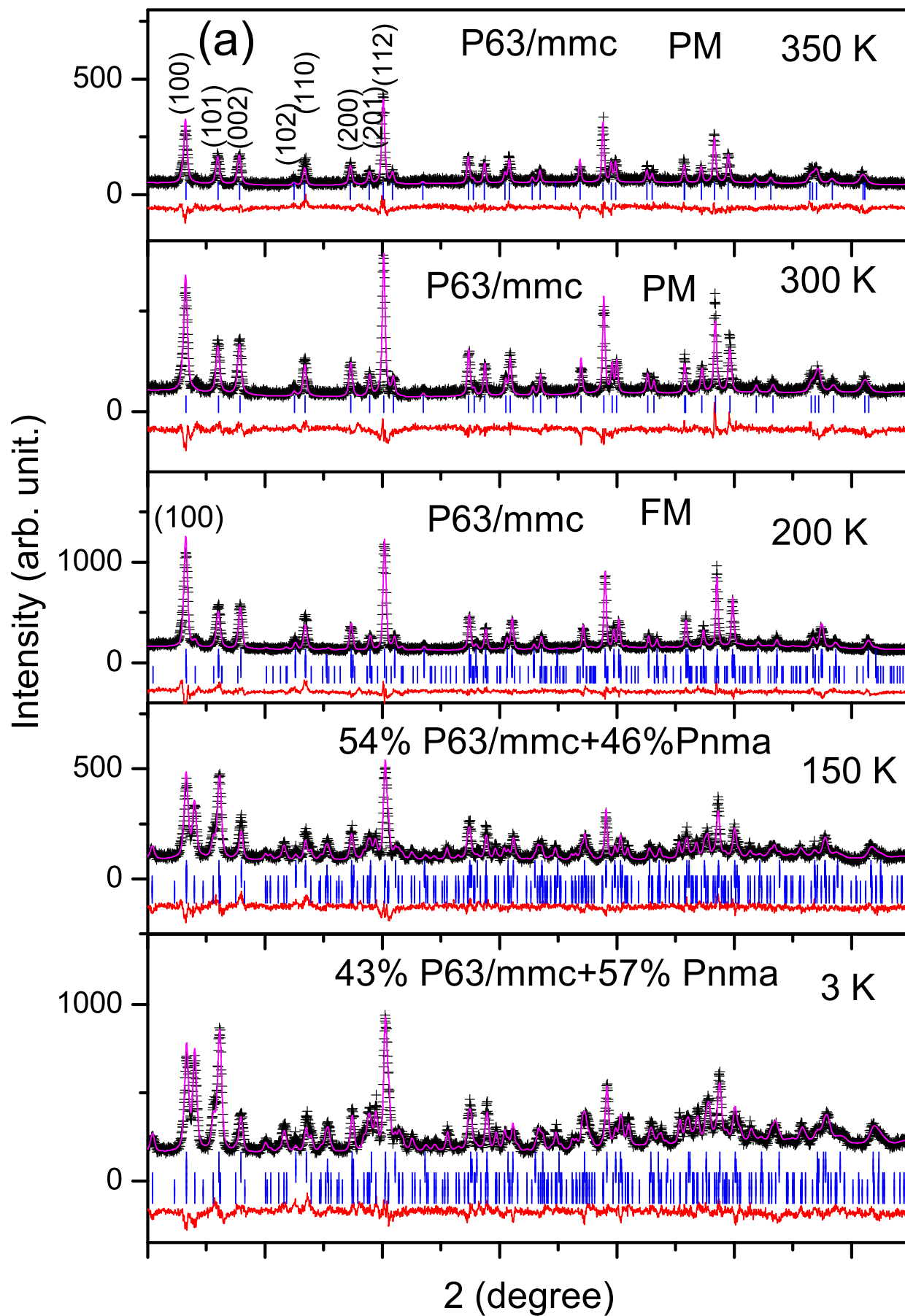




Figure(s)



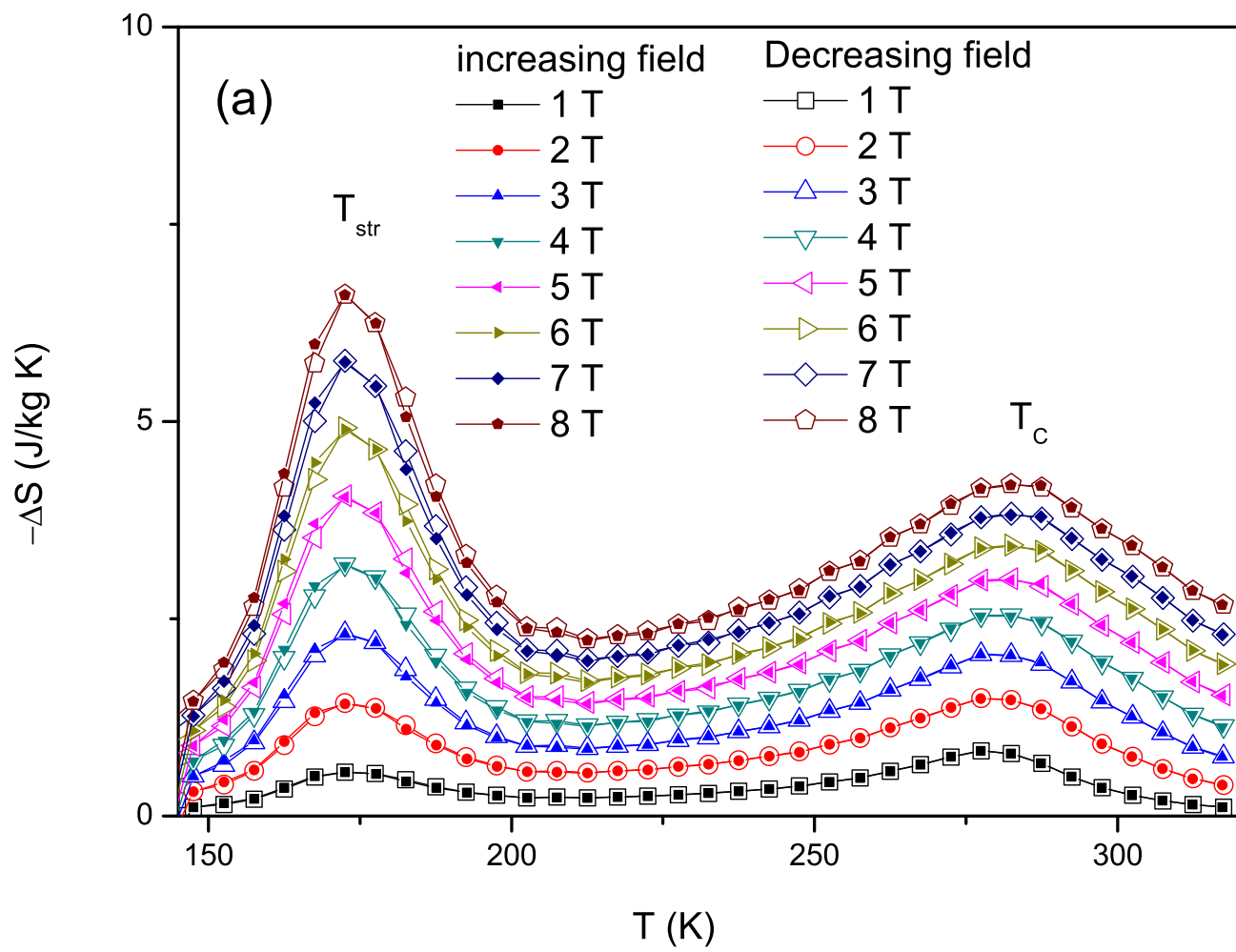
Figure(s)







Figure(s)



Figure(s)

